$^{16}O(\vec{p},\pi^+)^{17}O^*$ at incident proton energies of 250, 354, and 489 MeV

G. M. Huber, G. J. Lolos, and Z. Papandreou
Department of Physics and Astronomy, University of Regina, Regina, Saskatchewan, Canada S4S 0A2

K. H. Hicks, P. L. Walden, and S. Yen
TRIUMF, Vancouver, British Columbia, Canada V6T 2A3

R. D. Bent and G. T. Emery
Indiana University Cyclotron Facility, Bloomington, Indiana 47405

E. G. Auld and F. A. Duncan
Department of Physics, University of British Columbia, Vancouver, British Columbia, Canada V6T 2A6

W. R. Falk
Department of Physics, University of Manitoba, Winnipeg, Manitoba, Canada R3T 2N2
(Received 31 July 1987)

Differential cross sections and analyzing powers are presented for the $^{16}O(\vec{p},\pi^+)^{17}O^*$ reaction at $T_p=250$, 354, and 489 MeV and compared with preliminary 200 MeV data as well as previously published data taken at other energies above and below the Δ_{1232} resonance region. The differential cross sections for each final state exhibit an energy dependence similar to that of the $pp\rightarrow d\pi^+$ reaction at equivalent center of mass energy and four-momentum transfer, as has been seen previously for (p,π^+) reactions with other target nuclei. The shape of the analyzing power angular distributions varies with the $^{17}O^*$ nuclear final state. Some states exhibit broad similarities with that of the $\vec{p}p\rightarrow d\pi^+$ reaction, while others are markedly different.

I. INTRODUCTION

Over approximately the last 15 years, the exclusive (p,π^+) reaction has received sustained experimental and theoretical scrutiny.[1-4] Much of this interest has been because the reaction is characterized by a momentum transfer that is large compared to the nuclear Fermi momentum. Understanding how the nucleus coherently absorbs this large momentum transfer is important to the study of large momentum transfer processes in general. However, a key problem complicating the study of the (p,π^+) reaction has been the interplay between reaction mechanism and nuclear structure effects. Any hope of tapping the wealth of information hidden in the exclusive (p,π) reaction hinges on our ability to unravel the underlying reaction mechanism from the nuclear structure effects. Alternately, the large momentum transfer makes the (p,π^+) reaction a suitable spectroscopic tool for the study of previously unidentified high excitation states.[5,6]

Despite evermore sophisticated calculations of nuclear (p,π^+) reactions,[7-10] agreement between calculation and experiment is fragmentary. Systematic studies of a large number of cases will be necessary to gain a full understanding of the (p,π^+) reaction mechanism. Recent measurements of (p,π^+) differential cross-section and analyzing power distributions for transitions to many different final states[11-13] have begun to delineate the systematics of this reaction. Of particular importance are studies in the Δ_{1232} resonance region of reactions involving nuclei whose structure is known with some reliability; the $^{16}O(p,\pi^+)^{17}O$ reaction is such a case. In this energy region, signatures of the Δ_{1232} resonance, if present, should be the least ambiguous.

Except for a few older measurements near the threshold region,[14,15] and some preliminary data taken at LAMPF at 800 MeV,[16] there has not been an experimental survey of the $^{16}O(p,\pi^+)^{17}O^*$ reaction across a broad energy range. This scarcity of data is surprising because the closed shell nature of the ^{16}O nucleus simplifies theoretical calculations of this reaction. Experimental data on this target nucleus in the region of the Δ_{1232} invariant mass are necessary to confirm recently published systematics of the (p,π^+) reaction using other target nuclei of similar mass. In addition, no analyzing power measurements have ever been made for the $(\vec{p},\pi^+)$ reaction on nuclei with $A>2$ in this energy region; such measurements may aid in unravelling nuclear structure effects from the (p,π^+) reaction mechanism.

For the above reasons, we have studied the $^{16}O(p,\pi^+)^{17}O^*$ reaction using polarized proton beams of 250, 354, and 489 MeV, covering the energy range near the invariant mass of the Δ_{1232}. A simple calculation shows that the peak of the Δ_{1232} resonance should occur at $T_p=315$ MeV if the beam proton and ^{16}O target combine to form a mass 17 nucleus with one nucleon excited to a mass of 1232 MeV. To aid in understanding the energy dependent systematics of these reactions, we compare our results to preliminary 200 MeV data from an experiment recently completed at the Indiana University

Cyclotron Facility (IUCF),[6] as well as other previously published data.[14–16] In addition, we compare our data to a recent calculation of the $^{16}O(\vec{p},\pi^+)^{17}O_{g.s.}$ reaction across this energy range by Cooper and Matsuyama.[9] This is a modern relativistic stripping mechanism calculation, and our data should aid in the development of this, as well as other recently developed (p,π^+) models.[7,8,10]

II. THE EXPERIMENT

The experiment was performed with the medium resolution spectrometer (MRS) (Ref. 17) at TRIUMF using a polarized proton beam. The experimental procedure was essentially the same as that used in a previously published $^{12}C(p,\pi^+)^{13}C^*$ experiment performed on the MRS,[13] so only differences in procedure from that previous work will be explained.

Beam polarization was monitored continuously by an in-beam polarimeter located upstream of the experimental target. Beam polarization was typically 73% at 250 MeV, and approximately 60% at 354 and 489 MeV. Beam intensity was monitored by a secondary emission monitor (SEM), as well as with the in-beam polarimeter, both of which had been previously calibrated against a Faraday cup. The total charge on target readings given by the in-beam polarimeter were consistently higher than those given by the SEM by 17±4%. This deviation was consistent with that seen previously by other experimenters using the MRS,[18] and the stability of the ratio between the two beam normalizations leads one to believe that it was due to the thin polarimeter target, which has been known to wrinkle after an extended time period in the beam. Therefore, the SEM was used for the total charge on target, and we are confident that the beam normalization is accurate to within 2%, which is the accuracy of the SEM versus Faraday cup calibration.

Beam was incident on a $^7Li^{16}O^1H$ target of 100±1 mg/cm^2 thickness. In order to maximize the resolution of the MRS, the target angle with respect to the beam was chosen at each spectrometer angle setting so that the maximum energy loss of the proton beam in the target would be approximately equal to the maximum energy loss of the detected pions in the target. Because of reliability problems associated with the target angle readout system during the experiment, the uncertainty in the effective target thickness is estimated to be ±14%. This uncertainty was estimated by making two measurements at the same spectrometer angle and proton energy in which the target position and spectrometer angle were moved and then reset to their original positions. Any difference between the two measurements was attributed to the error in obtaining the original target position.

The location of events in the pion focal plane due to the $^7Li(p,\pi^+)^8Li^*$ reaction interfered with the most highly excited states in the $^{16}O(p,\pi^+)^{17}O^*$ reaction at only the most forward angles. At these angles, data from a 208±2 mg/cm^2 metallic ^7Li target were collected and subtracted from the $^7Li^{16}O^1H$ target data. These $^7Li(\vec{p},\pi^+)^8Li$ data have already been published.[19]

The spectrometer detection system consisted of a multiwire drift chamber located in front of the spectrometer's entrance quadrupole magnet, and two vertical drift chambers followed by two planes of plastic scintillators located near the focal plane of the spectrometer. The product of the efficiency of all three chambers was typically 88%, although at extreme back angles the product fell as low as 70%. This decrease in efficiency was shared equally between all three chambers, and was primarily due to the increased beam current used at back angles in order to reduce the running time, resulting in increased singles rates from background. The acquisition system live time varied between 83 and 98%, depending on the event rate.

The spectrometer acceptance was calibrated at 489 MeV using the $pp\rightarrow d\pi^+$ reaction, whose cross section is known to a precision of ±2%.[20] The proton energy for this calibration was chosen so that pions from this reaction would have approximately the same momentum as pions from the $^{16}O(p,\pi^+)^{17}O$ reaction at 354 MeV. The effective solid angle of the spectrometer, determined by this method, was 2.8 msr, which compares with the 3.0 msr geometric solid angle of the MRS spectrometer. The uncertainty of ±6% assigned to this solid angle determination is based on the accuracy to which the solid angle could be determined in previous experiments.[13] It does not include the 2% uncertainty in the $pp\rightarrow d\pi^+$ cross section itself and it also does not include the uncertainty in the integrated beam current.

The efficiency of the spectrometer focal plane was scanned using the $pp\rightarrow d\pi^+$ reaction by varying the spectrometer dipole magnetic field. A Legendre polynomial fit to the results of this scan allowed the efficiency of each focal plane coordinate to be calculated, and all net counts observed were corrected for the decrease in collection efficiency away from the center point. An uncertainty of 2%, incorporating the accuracy of this Legendre polynomial fit, has been assigned to this correction.

Systematic and relative errors for this experiment are summarized in Table I. The uncertainty quoted for the pion survival factor was based on the number of events located on the high momentum side of the $^{17}O_{g.s.}$ which can only be populated by muons via pion decay or pion

TABLE I. Sources of error, and their assigned values for this experiment.

Systematic uncertainties	
Solid angle	±6%
Pion survival factor	3%
Uncertainty in $pp\rightarrow d\pi^+$ calibration	2%
Target thickness	1%
Total systematic uncertainty	±7%
Relative uncertainties	
Effective target thickness	±14%
Maximum sensitivity to errors in the data analysis	8%
Aquisition system live time	4%
Integrated beam current	2%
Wirechamber efficiency	2%
Focal plane relative efficiency	2%
Total relative uncertainty	±17%

multiple scattering. The maximum uncertainty due to the inconsistent placement of cuts in the off-line, event-by-event analysis was estimated by analyzing some data twice, once with normal solid angle, beam spot, and particle trajectory cuts, and once with these cuts set drastically different. This test determined the maximum sensitivity of the differential cross sections presented here to errors in the data analysis.

III. RESULTS

Three off-line, event-by-event analyzed pion spectra (after solid angle, energy loss, time of flight, target beam spot, and particle trajectory cuts have been applied) are shown in Fig. 1. The energy resolutions for these spectra, as shown in Fig. 1, were 200 keV at 250 MeV, 165 keV at 354 MeV, and 225 keV at 489 MeV. The experimental resolution at each beam energy was due primarily to the energy spread of the proton beam as delivered from the TRIUMF cyclotron. The three spectra shown in Fig. 1 were taken at a fixed four momentum transfer of $t=0.45$ GeV$^2/c^2$. The states of ^{17}O which dominate all three spectra are the ground state $\frac{5}{2}^+$, and the 5.218 MeV ($\frac{9}{2}^-$), 7.757 MeV $\frac{11}{2}^-$, 15.78 MeV ($\frac{13}{2}^-$), and 17.1 MeV ($\frac{7}{2}^-$) excited states. Those spins which are within parentheses are only tentative assignments. We note that the strongly populated states have known, or tentatively assigned high spins, as expected from the large momentum transfer characteristic of this reaction. This selectivity for the population of high spin states is qualitatively similar to that seen for the (p,π^-) reaction at lower energies.[21]

Because of the small momentum acceptance of the MRS spectrometer, the 250 MeV spectrum shown in Fig. 1 is a composite of two separate momentum bites covering the full range of excitation energies shown. The broad high excitation peaks in the 354 and 489 MeV spectra are from the ^{7}Li$(p,\pi^+)^8$Li reaction due to the LiOH target; the 250 MeV spectrum has had contributions due to this reaction subtracted from it. These three spectra look very similar because they were all taken at the same four momentum transfer. The rough energy dependence of the reaction can be seen directly by comparing the y-axis scales in Fig. 1.

A peak fitting routine[22] was used to extract differential cross-section and analyzing power distributions for 23 different final states of the $^{17}O^*$ nucleus at each of the three energies. A spectrum showing a typical fit used to extract data for these 23 different states is shown in Fig. 2. The energy assignments for the stronger states labeled in Fig. 2 have an uncertainty of ± 50 keV, and have been taken from Ref. 23. Differential cross sections and analyzing powers for four of the more strongly populated states shown in Fig. 2 are listed in Table II; tables of data for all of these states, including the less strongly populated states, are available from the Physics Auxiliary Publication Service (PAPS) of the American Institute of Physics (AIP).[24]

A. Energy dependence of the differential cross sections

The differential cross sections for the $^{16}O(p,\pi^+)^{17}O^*$ reactions exhibit an energy dependence similar to that seen previously for several other (p,π^+) reactions.[13,25,26] Figures 3–7 show that at small momentum transfers ($t>0.45$ GeV$^2/c^2$) the differential cross section rises with energy from the pion production threshold up to the invariant mass of the Δ_{1232}, near $T_p=354$ MeV, and

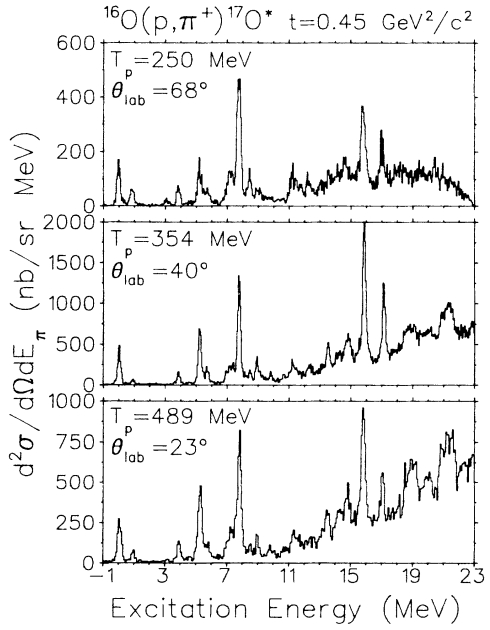

FIG. 1. Pion focal plane spectra after solid angle, energy loss, time of flight, target beam spot, and particle trajectory cuts.

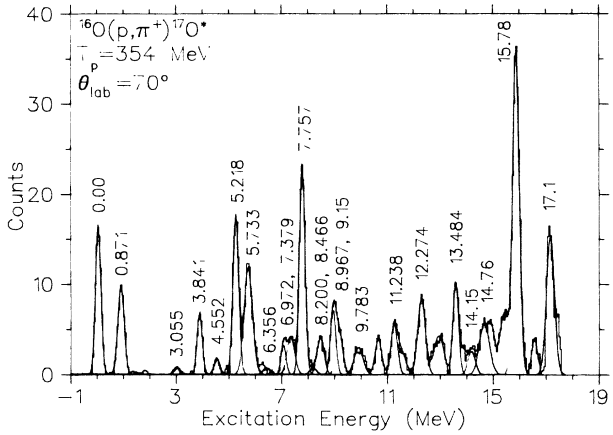

FIG. 2. Final result of peak fitting program (Ref. 22), showing all 23 final states of $^{17}O^*$ for which data have been extracted. The total fit to the spectrum, also shown here, included smaller peaks for which data have not been extracted. This spectrum has had background and contributions due to the continuum $^{16}O(p,\pi^+)X$ reactions subtracted from it, and was then smoothed by a cubic spline routine.

TABLE II. A list of differential cross sections and analyzing powers for the $^{16}O(\vec{p},\pi^+)$ reaction leading to four of the more strongly populated final states of $^{17}O^*$. All quantities shown are in the center of mass frame. Angles are in degrees, t is the square of the four momentum transfer in units of GeV$^2/c^2$, and the $d\sigma/d\Omega$ are in nb/sr. The numbers in parentheses reflect statistical uncertainties only.

$\theta_{c.m.}$	t	$^{17}O_{g.s.}$		$^{17}O^*_{5.218}$		$^{17}O^*_{7.757}$		$^{17}O^*_{15.78}$	
					$T_p=250$ MeV				
21	0.60	625(30)	−0.01(0.05)	416(24)	0.59(0.06)	1230(43)	0.19(0.04)	1860(83)	−0.18(0.04)
45	0.54	218(11)	−0.78(0.04)	212(10)	0.77(0.05)	501(16)	0.19(0.03)	712(25)	−0.10(0.03)
58	0.50	84.6(5.9)	0.30(0.07)	103(7)	0.67(0.05)	217(9)	−0.43(0.04)	438(17)	−0.07(0.04)
71	0.45	36.3(2.9)	0.66(0.08)	46.2(3.4)	0.30(0.08)	178(7)	−0.64(0.03)	195(7)	−0.03(0.03)
85	0.39	35.7(2.4)	−0.78(0.06)	46.3(2.9)	0.04(0.07)	99.6(4.4)	−0.19(0.05)	122(6)	−0.04(0.05)
102	0.32	39.9(2.3)	−0.76(0.05)	18.8(1.6)	0.12(0.09)	50.6(2.8)	0.27(0.05)	51.5(2.8)	0.32(0.05)
					$T_p=354$ MeV				
21	0.54	539(23)	0.14(0.04)	674(26)	0.20(0.04)	1740(42)	0.37(0.02)	1840(45)	0.12(0.03)
31	0.50	214(11)	0.41(0.05)	453(17)	0.16(0.04)	967(24)	0.41(0.03)	1110(27)	0.09(0.03)
42	0.45	112(5)	0.53(0.04)	162(5)	0.04(0.03)	307(8)	0.38(0.02)	476(10)	0.15(0.02)
52	0.39	45.4(3.5)	0.15(0.07)	57.1(4.0)	0.09(0.06)	96.9(5.2)	0.26(0.05)	188(8)	0.19(0.04)
58	0.34	20.8(2.1)	−0.52(0.10)	37.0(2.9)	−0.03(0.08)	51.1(3.4)	0.07(0.07)	116(6)	0.27(0.05)
63	0.31	12.5(0.9)	0.80(0.07)	24.2(1.2)	0.12(0.05)	31.0(1.4)	0.19(0.05)	61.4(2.1)	0.49(0.03)
73	0.23	7.0(0.8)	0.34(0.11)	8.2(0.8)	0.48(0.10)	11.1(1.0)	0.50(0.08)	22.4(1.5)	0.30(0.06)
83	0.15	5.9(0.6)	1.00(0.08)	2.3(0.3)	0.62(0.15)	4.8(0.5)	0.33(0.11)	8.6(0.7)	0.66(0.08)
					$T_p=489$ MeV				
24	0.45	77.4(5.0)	0.38(0.06)	144(7)	−0.12(0.05)	237(9)	−0.09(0.04)	275(10)	−0.10(0.04)
42	0.31	11.4(1.2)	−0.72(0.10)	17.4(1.5)	−0.50(0.09)	17.7(1.5)	−0.21(0.09)	34.4(2.2)	−0.48(0.06)
57	0.14	4.9(0.7)	0.88(0.13)	2.5(0.5)	−0.50(0.22)	3.1(0.6)	−0.17(0.21)	3.5(0.6)	0.09(0.19)

then falls slowly afterward. This feature is common to all (p,π^+) exclusive reactions studied so far, and has been attributed to the formation of an intermediate Δ_{1232} resonance via a comparison with the $pp\rightarrow d\pi^+$ reaction, which exhibits a similar feature at equivalent kinematical settings.[13] This comparison is valid because studying the energy dependence of the differential cross section at a constant four momentum transfer permits, in a first approximation, the decoupling of the reaction mechanism from nuclear structure effects.[25,26]

This energy dependence is shown in more detail in Fig. 8, which shows the energy dependence of the $^{16}O(p,\pi^+)^{17}O^*_{7.757}$ reaction more clearly. The quantity $\sqrt{s}-m_{^{16}O}$, where s is the relativistic Mandelstam variable corresponding to the square of the center of mass energy, is a measure of the excitation energy available for one nucleon. The Δ_{1232} invariant mass occurs at an x-axis value of 1.232 GeV. Also shown in this figure by the solid lines are the differential cross sections of the $pp\rightarrow d\pi^+$ reaction at equivalent center-of-mass energy and four momentum transfer transformed to the nuclear kinematical frame and normalized to the $^{16}O(p,\pi^+)^{17}O^*_{7.757}$ result. As can be seen for $t>0.45$ GeV$^2/c^2$, the $pp\rightarrow d\pi^+$ reaction exhibits a pronounced peak at the Δ_{1232} invariant mass as does the $^{16}O(p,\pi^+)^{17}O^*_{7.757}$ reaction. This can be interpreted as evidence for single nucleon excitation to the Δ_{1232}.

At much higher momentum transfers ($t<0.35$ GeV$^2/c^2$), the $pp\rightarrow d\pi^+$ reaction does not exhibit this enhancement, and we also note that at these four momentum transfers the 250 MeV $^{17}O^*_{7.757}$ data point ($\sqrt{s}-m_{^{16}O}=1.17$ GeV) has a larger differential cross section than either the 354 or 489 MeV $^{17}O^*_{7.757}$ data points. This energy dependence has been noted previously at large momentum transfers for other (p,π^+) reactions.[13] The $^{17}O^*_{15.78}$ state shown in Fig. 4, however, continues to show an enhancement at the Δ_{1232} invariant mass at these high momentum transfers. The $^{17}O^*_{0.871}$, $^{17}O_{g.s.}$ states shown in Figs. 5 and 6 exhibit pronounced large angle peaks at low beam energies which make their energy dependence at large momentum transfers very difficult to interpret.

Thus, at four momentum transfers $t>0.45$ GeV$^2/c^2$, most states exhibit an enhancement at the Δ_{1232} invariant mass which is similar to that exhibited by the $pp\rightarrow d\pi^+$ reaction after transformation to the nuclear kinematical frame. At larger momentum transfers ($t<0.35$ GeV$^2/c^2$), some states still exhibit an enhancement in differential cross section at the Δ_{1232} invariant mass, while other states do not show an enhancement, exhibiting instead a cross section that falls with energy from 250 to 489 MeV, similar to that shown for the $pp\rightarrow d\pi^+$ reaction in Fig. 8.

B. Spin dependence of the total cross section

It has been noted in Refs. 4 and 12 that the population of final states in the (p,π^+) reaction is roughly proportional to $2J_{A+1}+1$. Because of the large momentum transfer characteristic of (p,π^+) reactions, one would expect high angular momentum states to be prominent and saturated to their full $2J_{A+1}+1$ statistical weighting. This qualitatively describes the weak presence of low spin states in (p,π) reactions. Other high spin states

which are not strongly populated [e.g., $^{17}O^*_{14.15}(\frac{9}{2}^+)$] are presumably suppressed by some other mechanism, for example the nuclear structure of that state. Plotted in Fig. 9 is the reduced total cross section $(1/2J_{A+1}+1)\sigma$ for some of the most strongly populated states of ^{17}O. Also plotted for comparison, at the bottom of Fig. 9, are the total cross sections of these states. As Fig. 9 shows, the reduced total cross sections are indeed more clustered together than the total cross sections.

We also note that the total cross sections of the $^{16}O(p,\pi^+)^{17}O^*$ reactions shown in Fig. 9 do not peak at the invariant mass of the Δ_{1232}, but rather about 50–100 MeV lower than this, near 225 MeV. This energy dependence was observed previously in Ref. 13 for the $^{12}C(p,\pi^+)^{13}C^*$ reaction. As stated in this reference, the maxima of the total cross sections do not occur at the invariant mass of the Δ_{1232} because of an interplay between a rising cross section, due to the influence of the Δ_{1232} in the reaction mechanism, and a falling cross section due to the large momentum transfers that the exclusive (p,π^+) reaction is restricted to at higher energies.

C. Analyzing power distribution classifications

Analyzing powers for the states of $^{17}O^*$ do not have a common angular distribution, but fall into several broad categories.

1. *Category 1 ($pp \rightarrow d\pi^+$-like)*

The most common type of analyzing power distribution is one having a dip near $t=0.4$ GeV$^2/c^2$ at 250 MeV, a positive and fairly flat distribution at 354 MeV, and a negative flat analyzing power at 489 MeV. Almost half of the states studied had analyzing power distributions with this general pattern, of which the $^{17}O^*_{7.757}$ state shown in Fig. 3 is an example. Many of the states which exhibited this pattern are believed to be primarily of two-particle–one-hole (2p-1h) structure.

The analyzing power of the $^{16}O(\vec{p},\pi^+)^{17}O^*_{7.757}$ reaction, shown in Fig. 3, shares many similarities with the analyzing power of the $\vec{p}p\rightarrow d\pi^+$ reaction at equivalent center-of-mass energy and four momentum transfer. All other states in this category also had broad similarities to the analyzing power of the $\vec{p}p\rightarrow d\pi^+$ reaction, but the similarity was not as striking. As is clearly shown in Fig. 3, the 200 MeV analyzing power of the $^{16}O(\vec{p},\pi^+)^{17}O^*_{7.757}$ reaction is very similar to that of the basic $\vec{p}p\rightarrow d\pi^+$ reaction shown by the solid line (after the suitable kinematic transformation). This similarity has been noted several times before[11,31] for other target nuclei in this energy range.

At 250 MeV, the $^{17}O^*_{7.757}$ state exhibits a much more negative dip in the analyzing power than the $\vec{p}p\rightarrow d\pi^+$ reaction, and the minimum for the $\vec{p}p\rightarrow d\pi^+$ reaction occurs at slightly lower t value. At 354 MeV, the analyzing powers for both reactions turn positive and have approximately the same magnitude, although the $^{16}O(\vec{p},\pi^+)^{17}O^*_{7.757}$ reaction displays a dip at $t=0.35$ GeV$^2/c^2$ which is not evident in the $\vec{p}p\rightarrow d\pi^+$ data. At

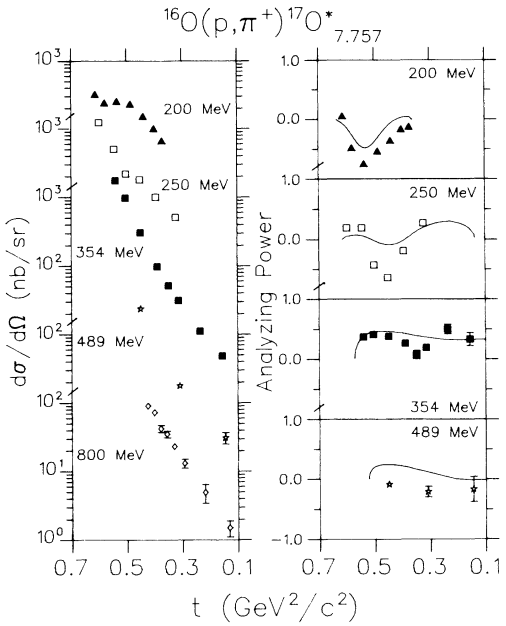

FIG. 3. Differential cross sections and analyzing powers for the $^{16}O(\vec{p},\pi^+)^{17}O^*_{7.757}$ reaction. The preliminary 200 MeV data are from Ref. 6, the 250, 354, and 489 MeV data are from this work, and the preliminary 800 MeV data are from Ref. 16. The smooth line is the analyzing power of the $\vec{p}p\rightarrow d\pi^+$ reaction based on the polynomial fits of Refs. 20 and 27–30 with the appropriate kinematical transformation to the nuclear frame. Differential cross sections are not displayed on a common scale for sake of clarity.

489 MeV, analyzing powers for the $^{17}O^*_{7.757}$ reaction once again become negative, while those for the $\vec{p}p\rightarrow d\pi^+$ reaction remain positive. Clearly, the evidence for an underlying $\vec{p}p\rightarrow d\pi^+$ mechanism in the $^{17}O^*_{7.757}$ reaction is stronger at 200 MeV than at the higher energies, although the two nucleon process qualitatively describes the data up to 354 MeV.

2. *Category 2 (flat at forward angles)*

The next most common type of analyzing power angular distribution is exemplified by the $^{17}O^*_{15.78}$ state in Fig. 4 and by the $^{17}O^*_{17.1}$ state. These analyzing power distributions are flatter at forward angles than any of the other distributions shown elsewhere in this paper (perhaps with the exception of the $^{17}O^*_{5.218}$ state shown in Fig. 7), and are similar to the flat analyzing powers reported for two other high excitation states by Ref. 5. The nuclear structure configuration of most of the states which exhibit this type of analyzing power pattern is unknown. Despite the difference between the shape of these distributions, and those in category 1, we once again observe that the mainly negative analyzing powers at 200 MeV become positive by 354 MeV and then become negative again at 489 MeV.

3. *Category 3 (oscillating above 250 MeV)*

The third type of analyzing power distribution has large oscillations from 250 to 489 MeV, as shown by the

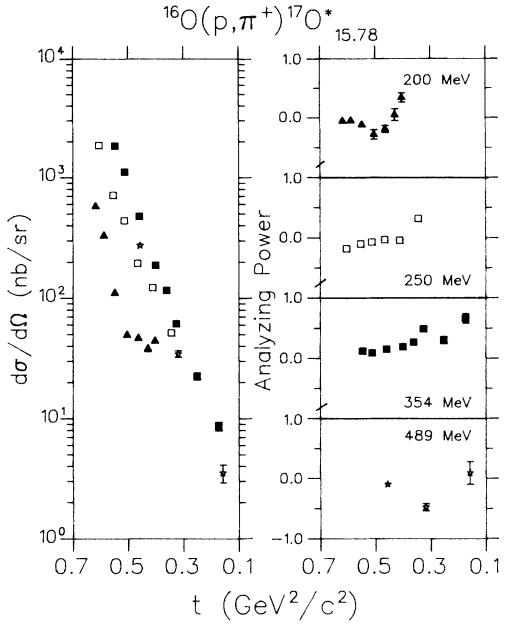

FIG. 4. Differential cross sections and analyzing powers for the $^{16}O(\vec{p},\pi^+)^{17}O^*_{15.78}$ reaction. All data shown are from this work except the preliminary 200 MeV data from Ref. 6.

$^{17}O^*_{0.871}$ state in Fig. 5. The 250 MeV analyzing power distribution shown in this figure has a negative forward angle dip which is not visible in Fig. 3. Thus, the frequency of the 250 MeV analyzing power oscillation in Fig. 5 is much larger than the frequency of the 250 MeV analyzing power oscillation in Fig. 3. Data for other states not shown in this paper at higher excitation have less dramatic analyzing power oscillations. Many of the states which exhibited this type of analyzing power distribution were primarily of single particle (1p) or three-particle–two-hole (3p-2h) structure. Once again we see that the analyzing powers at 354 MeV are generally more positive than those at 250 and 489 MeV.

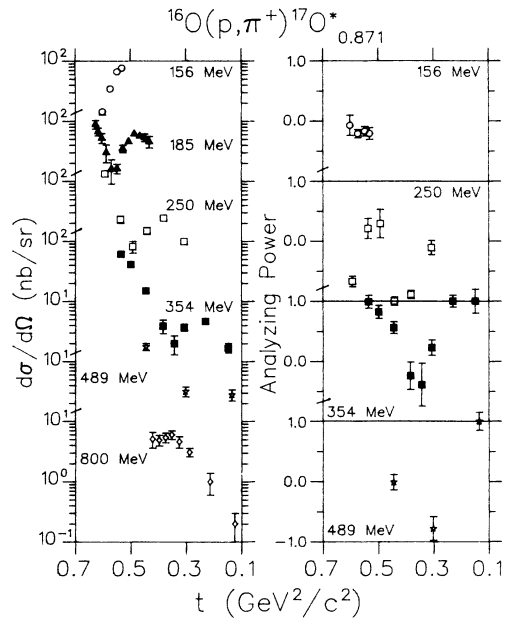

FIG. 5. Differential cross sections and analyzing powers for the $^{16}O(\vec{p},\pi^+)^{17}O^*_{0.871}$ reaction. The 156 MeV data are from Ref. 15, the 185 MeV data are from Ref. 14, the 250, 354, and 489 MeV data are from this work, and the preliminary 800 MeV data are from Ref. 16. Differential cross sections are not displayed on a common scale for sake of clarity.

4. *Exceptions*

Two states which do not seem to follow any of the previously described patterns are the $^{17}O_{g.s.}$ and $^{17}O^*_{5.218}$ states. As shown in Fig. 6, the ^{17}O ground state has a rapidly oscillating analyzing power at all energies from threshold, at 156 MeV, to well above the Δ_{1232} invariant mass, at 489 MeV. This type of energy dependence was not displayed by any other state studied in this paper. Although the analyzing power oscillations exhibited by this state at 250, 354, and 489 MeV are very similar to that of the $^{17}O^*_{0.871}$ state shown in Fig. 5, it should be noted that at 250 MeV the oscillations of the $^{17}O_{g.s.}$ are about a quarter oscillation out of phase with the oscillations of the $^{17}O^*_{0.871}$ state, while the two analyzing power distributions appear to oscillate with the same frequency. Nevertheless, the two states have very different low energy analyzing power distributions.

The other state which does not seem to fall in any of these analyzing power categories is the $^{17}O^*_{5.218}$ state shown in Fig. 7. The analyzing powers for this state are

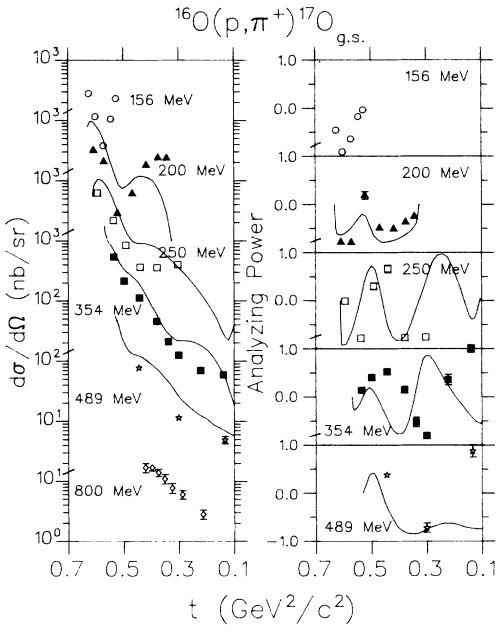

FIG. 6. Differential cross sections and analyzing powers for the $^{16}O(\vec{p},\pi^+)^{17}O_{g.s.}$ reaction. The 156 MeV data are from Ref. 15, the preliminary 200 MeV data are from Ref. 6, the 250, 354, and 489 MeV data are from this work, and the preliminary 800 MeV data are from Ref. 16. Also shown by the solid lines is a relativistic stripping model calculation by Cooper and Matsuyama[9] at 200, 250, 350, and 450 MeV. Differential cross sections are not displayed on a common scale for sake of clarity.

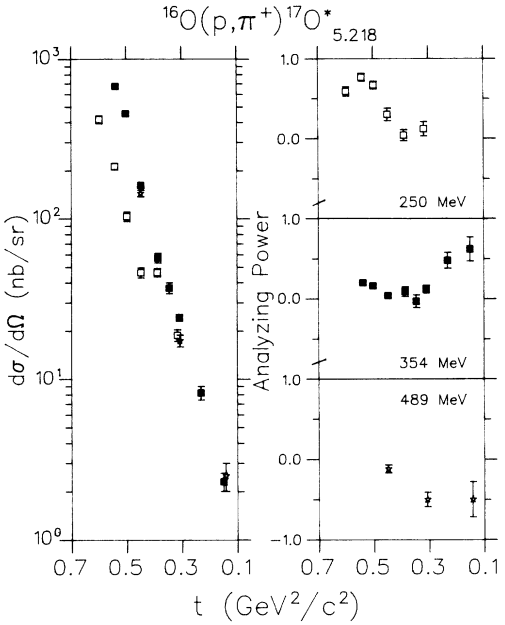

FIG. 7. Differential cross sections and analyzing powers for the $^{16}O(\vec{p},\pi^+)^{17}O^*_{5.218}$ reaction. All data shown are from this work.

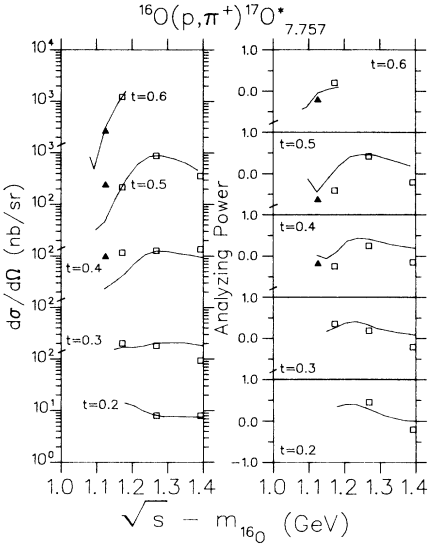

FIG. 8. Differential cross sections and analyzing powers for the $^{16}O(\vec{p},\pi^+)^{17}O^*_{7.757}$ reaction plotted against the center of mass energy ($\sqrt{s} - m_{^{16}O}$). Plotting symbols indicate the source of data as follows: ▲ (Ref. 6) 200 MeV; □ (this work) 250, 354, and 489 MeV. Plotted differential cross sections were calculated using Legendre polynomial fits to the data; plotted analyzing powers were calculated using associated Legendre polynomial fits to the data. The solid lines are the differential cross sections and analyzing powers of the $\vec{p}p\rightarrow d\pi^+$ reaction based on the polynomial fits of Refs. 20 and 27–30 with the appropriate kinematical transformation to the nuclear frame and referred to the nucleon-nucleus center of mass frame. The $pp\rightarrow d\pi^+$ differential cross sections have been normalized to the 354 MeV $^{17}O^*_{7.757}$ data point, except at $t=0.6$ GeV^2/c^2, which was normalized to the 250 MeV data point.

entirely positive at 250 MeV, positive but on average of smaller magnitude at 354 MeV, and entirely negative at 489 MeV.

In summary, the analyzing power angular distributions of many 2p-1h states have some resemblance to those of the $\vec{p}p\rightarrow d\pi^+$ reaction. However, there are also many states of differing nuclear structure which have entirely different analyzing power distributions. This variety of analyzing power shapes has been observed previously in $(\vec{p},\pi^+)$ reactions in only a few isolated cases.[5]

D. Energy dependence of the analyzing powers

In Fig. 8 the energy dependence of the analyzing power for the $^{16}O(\vec{p},\pi^+)^{17}O^*_{7.757}$ reaction is shown at several different four momentum transfers. The energy dependence of the analyzing powers for this reaction is better described by the $\vec{p}p\rightarrow d\pi^+$ curves shown by the solid lines in the same figure than those of the differential cross sections. We note that in the region $t>0.35$ GeV^2/c^2 both the $^{16}O(\vec{p},\pi^+)^{17}O^*_{7.757}$ reaction and the $\vec{p}p\rightarrow d\pi^+$ reaction have an analyzing power energy dependence in which the analyzing power is most positive near the Δ_{1232} invariant mass. This could be interpreted as another signature that is consistent with the characteristics of a $NN\rightarrow NN\pi^+$ process.

As previously noted in Sec. III C, there is a tendency for many states to have analyzing powers which are more positive at 354 MeV than at 250 and 489 MeV (with the exception of the $^{17}O^*_{5.218}$ state shown in Fig. 7). We also note that the forward angle $(\vec{p},\pi^+)$ analyzing power data obtained at even higher energies are exclusively negative.[33–35] Although this is qualitatively similar to the behavior shown in Fig. 9 (for bombarding energies up to 500 MeV), the analyzing power energy

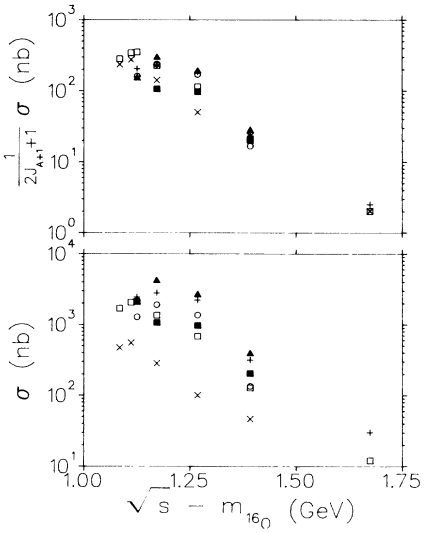

FIG. 9. Reduced total cross section, as explained in the text, as well as the total cross section for the $^{16}O(p,\pi^+)$ reaction leading to several different states of $^{17}O^*$. Plotting symbols indicate the final state of $^{17}O^*$ as follows: □, $^{17}O_{g.s.}$ ($\frac{5}{2}^+$); ×, $^{17}O^*_{0.871}$ ($\frac{1}{2}^+$); ■, $^{17}O^*_{5.218}$ ($\frac{9}{2}^-$); +, $^{17}O^*_{7.757}$ $\frac{11}{2}^-$; ▲, $^{17}O^*_{15.78}$ ($\frac{13}{2}^-$); ○, $^{17}O^*_{17.1}$ ($\frac{7}{2}^-$). The spin assignment for the 15.78 MeV state was taken from Ref. 32.

dependence of these other states does not resemble the $\vec{p}p \rightarrow d\pi^+$ reaction so clearly. The striking similarity to the $\vec{p}p \rightarrow d\pi^+$ reaction in Fig. 8 may be because the $^{17}O^*_{7.757}$ state is primarily a stretched 2p-1h state to which only two nucleon processes can contribute. For the other states, their nuclear structure could allow greater contributions from stripping, and other processes, masking the contribution of the two nucleon processes.

E. Comparison of data with theoretical calculations

Plotted in Fig. 6 are relativistic stripping model calculations for the $^{16}O(\vec{p},\pi^+)^{17}O_{g.s}$ reaction by Cooper and Matsuyama[9] which are compared with differential cross-section and analyzing power data from the present work and Ref. 6. The calculation by Cooper and Matsuyama is a relativistic stripping model calculation which uses the Dirac impulse approximation for the incoming proton-nucleus interaction, Dirac-Hartree wave functions for the neutron bound state, and a Δ-hole potential for the outgoing pion-nucleus distortions. All parameters used in this calculation are constrained by previous experiments, and its normalization is absolute.

Comparing the differential cross-section calculations with the experimental data, we see that the agreement between theory and experiment is superior at 354 MeV, and worse at energies far below the invariant mass of the Δ_{1232} (200, 250 MeV). This behavior is in contrast to the earlier relativistic stripping model calculations of Cooper and Sherif[36] in which agreement between data and calculation was fairly good for energies below 185 MeV. Since the only difference between these two models is in the use of the Δ-hole potential, rather than a local Stricker, McManus, and Carr potential for the outgoing pion distortions, this must be the cause of the improved agreement in the Δ_{1232} region. In fact, as shown in Ref. 9, a local potential calculation at 350 MeV overestimates the 354 MeV experimental data by approximately one order of magnitude. Thus, the differential cross section for the local potential calculation rises rapidly with energy, and only agrees with experimental data at energies fairly close to pion production threshold. The Δ-hole potential calculation, on the other hand, overestimates the 200 MeV differential cross section and rises much more slowly with energy.

Figure 6 also shows that the Δ-hole potential calculation of Ref. 9 qualitatively predicts the oscillations of the analyzing power data. Here, the agreement between data and calculation is clearly superior at 200 MeV rather than at the higher energies. In particular, the calculations at 250 and 350 MeV are out of phase with the data, and the calculation at 450 MeV completely fails to reproduce the continued oscillations of the 489 MeV data. We note that the local potential calculation at 350 MeV greatly underestimates the magnitude of the analyzing power oscillations, and has the wrong frequency of oscillation as well. The authors of this model are unable, at present, to account for the failure to predict the oscillations at 489 MeV, or for the error in phase in the 250 and 350 MeV analyzing power calculations. Nevertheless, this model has been the most successful to date in qualitatively describing some experimental data over a large energy range.

IV. SUMMARY AND CONCLUSIONS

In summary, we have investigated the energy, momentum transfer, and spin dependence of the $^{16}O(\vec{p},\pi^+)$ reaction leading to several states of $^{17}O^*$. Differential and total cross sections for many of these states behave in a manner consistent with previously reported data[13,25] for other (p,π^+) reactions in this energy range. In particular, at small momentum transfers ($t > 0.45$ GeV$^2/c^2$) most states exhibit an enhancement in differential cross section at the Δ_{1232} invariant mass which is similar to that exhibited by the $pp \rightarrow d\pi^+$ reaction after transformation to the nuclear kinematical frame. At larger momentum transfers ($t < 0.35$ GeV$^2/c^2$), some states continue to display an enhancement at the Δ_{1232} invariant mass, but other states exhibit a different energy dependence in which the differential cross section falls with energy from 250 to 489 MeV. This second type of energy dependence is similar to that displayed by the $pp \rightarrow d\pi^+$ reaction at large momentum transfer. Although this energy dependence could imply the dominance of the Δ_{1232} resonance in the (p,π^+) reaction mechanism, interpretation of this result is complicated by the differing energy dependences at large momentum transfer exhibited by various final states.

The analyzing power measurements are the first taken in this energy range, and also display some similarities to those of the $\vec{p}p \rightarrow d\pi^+$ reaction after the appropriate kinematical transformation to the nuclear frame. In particular, at four momentum transfers of $t > 0.35$ GeV$^2/c^2$, the energy dependence of the analyzing power for many final states is broadly similar to that of the $\vec{p}p \rightarrow d\pi^+$ reaction. This finding could be interpreted as a signature of the underlying $NN \rightarrow NN\pi^+$ reaction mechanism, but is once again complicated by the differing energy dependences exhibited by various final states.

A relativistic stripping model calculation for the $^{16}O(\vec{p},\pi^+)^{17}O_{g.s.}$ transition by Cooper and Matsuyama[9] is the first (p,π^+) calculation to be applied over such a broad energy range. It has moderate success in describing the data.

ACKNOWLEDGMENTS

The authors would like to thank C. A. Miller for his help with the spectrometer and D. Frekers for his help with the updated analysis program. We especially thank S. M. Aziz for sharing some of his preliminary 200 MeV data with us. This experiment was funded by a grant from the Natural Sciences and Engineering Research Council of Canada (NSERC).

[1]D. F. Measday and G. A. Miller, Annu. Rev. Nucl. Part. Sci. **29**, 121 (1979).
[2]B. Hoistad, *Advances in Nuclear Physics,* edited by J. W. Negele and E. Vogt (Plenum, New York, 1979), Vol. 11, p. 135; B. Hoistad, *Pion Production and Absorption in Nuclei—1981 (Indiana University),* Proceedings of the Workshop on Pion Production and Absorption in Nuclei, AIP Conf. Proc. No. 79, edited by R. D. Bent (AIP, New York, 1982), p. 105.
[3]H. W. Fearing, Progress in Particle and Nuclear Physics, edited by D. Wilkinson (Pergamon, New York, 1981), Vol. 7, p. 113.
[4]P. Couvert, Proceedings of the Workshop on Studying Nuclei with Medium Energy Protons, Edmonton, 1983, TRIUMF Report No. TRI-83-3, 1983, p. 287.
[5]E. Korkmaz *et al.*, Phys. Rev. Lett. **58**, 104 (1987).
[6]S. M. Aziz (private communication); S. M. Aziz *et al.*, Bull. Am. Phys. Soc. **32**, 1062 (1987).
[7]B. D. Keister and L. S. Kisslinger, Nucl. Phys. **A412**, 301 (1984).
[8]M. J. Iqbal and G. E. Walker, Phys. Rev. **32**, 557 (1985).
[9]E. D. Cooper and A. Matsuyama, Nucl. Phys. **A460**, 699 (1986).
[10]P. W. F. Alons, R. D. Bent, J. S. Conte, and M. Dillig, Nucl. Phys. (to be published).
[11]G. J. Lolos *et al.*, Phys. Rev. C **25**, 1086 (1982); **30**, 574 (1984).
[12]W. A. Ziegler *et al.*, Phys. Rev. C **32**, 301 (1985); W. A. Ziegler, Ph.D. thesis, University of British Columbia, 1985.
[13]G. M. Huber *et al.*, Phys. Rev. C **36**, 1058 (1987).
[14]S. Dahlgren, P. Grafstrom, B. Hoistad, and A. Asberg, Nucl. Phys. **A227**, 245 (1974).
[15]T. P. Sjoreen *et al.*, Phys. Rev. C **24**, 1135 (1981); **24**, 2569 (1981); T. P. Sjoreen, Scientific Technical report, 1980.
[16]H. Nann, *Pion Production and Absorption in Nuclei—1981 (Indiana University),* Proceedings of the Workshop on Pion Production and Absorption in Nuclei, AIP Conf. Proc. No. 79, edited by R. D. Bent (AIP, New York, 1982), p. 219.
[17]C. A. Miller, Proceedings of the Workshop on Studying Nuclei with Medium Energy Protons, Edmonton, 1983, TRIUMF Report No. TRI-83-3, 339 (1983).
[18]D. Frekers (private communication).
[19]G. M. Huber *et al.*, Phys. Rev. C **36**, 2683 (1987).
[20]G. L. Giles, Ph.D. thesis, University of British Columbia, 1985.
[21]T. G. Throwe *et al.*, Phys. Rev. C **35**, 1083 (1987).
[22]J. W. Rowson, Ph.D. thesis, University of Regina, 1978.
[23]F. Ajzenberg-Selove, Nucl. Phys. **A460**, 1 (1986).
[24]See AIP document No. PAPS PRVCA-37-215-04 for four pages of data on differential cross section and analyzing powers. Order by PAPS number and journal reference from American Institute of Physics, Physics Auxiliary Publication Service, 335 East 45th Street, New York, N.Y. 10017. The prepaid price is $1.50 for a microfiche, or $5 for a photocopy. Airmail additional.
[25]P. Couvert and M. Dillig, Abstracts International Conference on High Energy Physics and Nuclear Structure, Versailles (1981), p. 192.
[26]G. M. Huber *et al.*, Submitted to Phys. Rev. C (in press).
[27]E. L. Mathie *et al.*, Nucl. Phys. **A397**, 469 (1983).
[28]A. Saha *et al.*, Phys. Rev. Lett. **51**, 759 (1983).
[29]J. Hofteizer *et al.*, Nucl. Phys. **A402**, 429 (1983); **A412**, 286 (1984).
[30]B. Mayer *et al.*, Nucl. Phys. **A437**, 630 (1985).
[31]E. G. Auld *et al.*, Phys. Rev. C **25**, 2222 (1982); Phys. Rev. Lett. **41**, 462 (1978).
[32]C. L. Blilie *et al.*, Phys. Rev. C **30**, 1989 (1984).
[33]B. Hoistad *et al.*, Phys. Rev. C **29**, 553 (1984).
[34]B. Hoistad *et al.*, Phys. Lett. **177B**, 299 (1986).
[35]K. K. Seth, R. Soundranayagam, and B. Parker, LAMPF Annual Report, 1986, p. 35.
[36]E. D. Cooper and H. S. Sherif, Phys. Rev. C **25**, 3024 (1982); E. D. Cooper, Ph.D. thesis, University of Alberta, 1981.